



Presented at GNSS 2004  
The 2004 International Symposium on GNSS/GPS

Sydney, Australia  
6–8 December 2004

## Nominal Signal Deformations: Limits on GPS Range Accuracy

***R. E. Phelts***

Stanford University,  
Department of Aeronautics and Astronautics  
Durand Bldg., Room 060  
Stanford California 94305

Tel: (650) 724-7139 Fax: (650) 725-5517 Email: pheltsre@stanford.edu

***D. M. Akos***

University of Colorado  
101 ECAE – Aerospace Engineering Sciences  
429 UCB  
Boulder, CO

Tel: (303) 735-2187 Fax: (303) 492-7881 Email: dma@colorado.edu

### **Presenter Name(s)**

R. Eric Phelts

### **ABSTRACT**

Satellite-based navigation requires precise knowledge of the structure of the transmitted signals. For GPS, accurate knowledge of the shape of the ranging codes is required to ensure no biases are introduced into the position solution. It is generally presumed that all GPS-like satellite signals were virtually identical, however new research has shown that there may be significant variations between different GPS satellite signals. Since most GPS receivers require signals from four or more satellites, many GPS navigation solutions (past, present, and future) may contain unexplained bias errors ranging from a few centimeters to several meters.

Current GPS receivers presume GPS signals are identical and that range errors result solely from atmospheric effects, clock errors and multipath. In fact, this type of error, if present, is likely often mistaken for multipath. However, a separate error may result from non-uniform signal distortion between GPS signals. This error is believed to result from small filter group delay variations between satellite transmission antennas. Accordingly, ranging accuracy may more-heavily depend on factors such as receiver front-end filtering and correlator spacing.

This paper presents high-resolution, low-noise measurements to directly compare the received signals from various satellites. It is shown that GPS signals may differ significantly from one to another. Also, it proposes that ranging accuracy may have fundamental limitations not related to the usual

random, noise-like error sources discussed in previous papers. Further, it is concluded that high-integrity augmentation systems such as WAAS and LAAS—which attempt to protect wide range of receiver types—may need to take additional steps to limit the impact of these errors on aviation users.

**KEYWORDS:** signal, deformation, distortion, filters, group delay, GEO, bias, nominal, correlation peak, range error

## 1. INTRODUCTION

It is well-known that signal distortions or deformations cause range errors. Many have been studied and analyzed by many in the past. Multipath is a form of signal deformation that acts similar to the effects discussed in this paper. Its effect on GPS ranging capability has been extensively analyzed for many years. Signal deformations caused by satellite failures are somewhat less well-known; however these too have been analyzed and quantified in the past. (Phelts *et al.* 2000; Macabiau and Chatre 2000; Edgar *et al.*, 2000).

The effects of nominal signal distortions on ranging performance have much more recently become of interest to the navigation community. The Wide Area Augmentation System (WAAS) employs geostationary satellites (GEOs) for datalink and ranging purposes that have significantly different filter characteristics than GPS satellites. This difference, along with filter and tracking disparities between the reference and user receivers have been found to lead to potentially significant range biases (Phelts *et al.*, 2004). The Local Area Augmentation System (LAAS) does not rely on GEO measurements. Still, its more-stringent range accuracy requirements make the results of this type of analysis extremely pertinent for navigation using GPS satellites alone.

In practice, it is quite challenging to both observe and identify biases from nominal signal deformations. Position errors, range errors and correlation peak distortions are their effects. Position domain measurements are easiest to obtain and to process; correlation peak measurements are perhaps the most difficult. Despite this, these kinds of biases are most-difficult to observe in the position domain and are least hidden in the correlation domain.

In the position domain, its effects are very similar to slowly-varying multipath. The number of satellites tracked and their varying geometries generally cause the position error biases to slowly vary with time. And, since multipath (and any residual atmospheric error) is always present to some degree on each code range measurement, some of the errors attributed to multipath, may actually be due to these nominal biases. In the range domain, errors from nominal biases are virtually indistinguishable from static multipath. Special measures must be taken (e.g., using a high-gain, directional antenna) to identify them. The directional antenna, of course, then limits the number of space vehicles (SVs) that can be observed at any given time. Correlation domain techniques—the approach taken in this paper—require more-specialized receiver hardware in addition to the antenna requirements; however, they provide the most flexible means of observing the biases.

This paper uses methods and tools developed for GEO bias determination and satellite signal deformations to uncover the nominal distortions present on GPS satellites. Some of this work has been done by Mitelman (2005) and is briefly summarized in Section 2.4.1. As employed by Mitelman (2005), the work here also combines high-gain antenna measurements with a high-resolution signal analyzer and a software radio receiver. Additionally, this analysis takes

a comprehensive look at the output several of the GPS satellites through the use of correlation peak comparisons—measurements that directly translate to user ranging performance. This paper quantitatively compares the ranging performance of these satellites to ideal, theoretical predications and to each other.

## **2. CODE CORRELATION AND GPS ERROR SOURCES**

The autocorrelation of ideal C/A pseudorandom noise (PRN) codes form perfect, triangular correlation peaks. For the current GPS constellation (consisting of 32 distinct PRNs) and the current two Inmarsat GEO PRNs, the slopes of those peaks may have three nominal values (Phelts, 2001). However, the peaks are perfectly symmetric and are effectively identical from SV-to-SV. (The slopes of the correlation peaks need not be identical from PRN-to-PRN, or rather SV-to-SV. Provided the correlation peaks are symmetric, the discriminator curves will share a common zero-crossing.) Traditional analyses presume this is the correct model for the satellite signal as transmitted by GPS satellites.

Throughout this paper, range errors will be discussed in terms of their effect on the correlation peak. GNSS error sources affect correlation peaks in different ways. Some produce position errors, others do not; they may produce timing errors instead. Some are present all of the time and others vary with time and still others only occur under failure conditions. The subsections below briefly describe many of these and their affect on correlation peaks.

### **2.1 Atmospheric Errors**

The ionosphere and troposphere cause ranging biases. They effectively cause a shift in the correlation peak that is not accompanied by asymmetry. Higher-order effects of the ionosphere may cause negligible correlation peak distortion.

### **2.2 Timing Errors**

Timing errors exist nominally due to the nature of most (imprecise) receiver clocks, which must be calibrated using GPS. In addition to this, however, residual errors in the satellite clock may exist. Also, the satellite clock may fail and cause a particular range solution to drift off until the problem is corrected by the Ground Control Segment. These effects cause range biases that manifest themselves as shifts in the correlation peak; they do not cause correlation peak distortion. If the error is in the receiver clock, the result is an effective uniform shift of all received signals or correlation peaks that does not lead to range or position errors.

### **2.3 Receiver Filtering**

If the satellite signals are effectively matched from SV-to-SV, any filtering performed by the front ends of GPS receivers will affect all incoming signals identically. Since front end filters, in general, do not have perfectly linear phase, they do create some amount of correlation peak asymmetry. Still, provided all receiver correlator spacings are identical in a given receiver, this will translate into a uniform bias, or correlation peak shift, across all range

measurements. This bias will be solved for in the navigation solution and will not affect code positioning accuracy. If, however, the satellite signals are not identical from SV-to-SV, range errors may exist and adversely affect the navigation solution. This latter case is discussed further in the next subsection.

## 2.4 Signal deformations

For the purposes of this paper, signal deformations are defined as distortions of the signal that cause the peak itself to become, in general, asymmetric. These may result from either thermal noise, multipath, satellite failures or filter effects (e.g., filter group delay response) or some combination thereof. Whenever these distortions occur, they are generally not identical on all incident signals. Unpredictable range errors are often the result.

Multipath and thermal noise, of course, are always present to some extent. Satellite failures, such as the type that affected SV19 in 1993, are rarer (Edgar *et al*, 2000). These have since been modeled as in Figure 1 (Phelts *et al*, 2000). Filter distortions generally occur due to the presence of analog components in the signal chain. They are caused by group delay variations (i.e., non-linear phase) across the passband of a given filter. The filters may be those on the transmission path of the satellite signal or in the front end of the receiver. This too leads to range biases that affect identical signals the same. However, if the satellite transmission path filters are not identical they will cause the respective signals to differ. If the signals differ, then the receiver filter will accordingly modify them in slightly different ways.

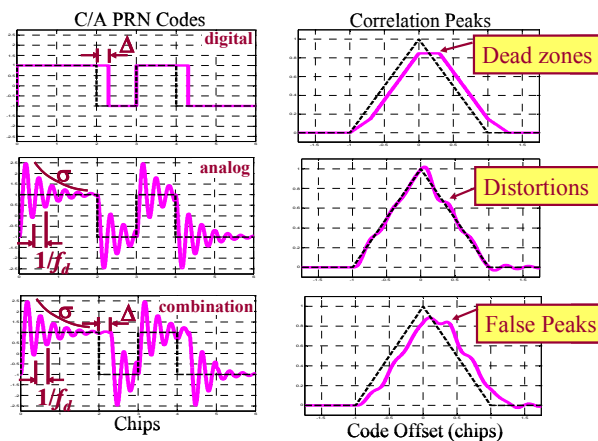


**Figure 1.** A depiction of the accepted code and correlation models for satellite signal deformation failures. More details on this model are provided by Phelts (2001).

The WAAS GEO signal is a notable example of the result of a filter-induced, nominal signal deformation. The current WAAS geostationary satellites broadcast narrowband (2.2MHz) ranging signals. The filters on the GEO signal path have characteristics which differ significantly from that of the GPS signals. The transmitted signals are deformed differently than are GPS signals; a given receiver processes them slightly differently. Substantial range biases may result if proper mitigation measures are not taken (Phelts *et al*, 2004).

### 2.4.1 PRN Code Domain Observations

The raw GPS PRN codes themselves, as generated, are not ideal. If the rise and fall times of the chip transitions are not matched, an ideal correlation peak may develop a small “dead zone” distortion. This type of distortion is illustrated in the first plot of Figure 1. This effect and the measurement techniques used to precisely measure the raw PRN codes are more completely described by Mitelman (2005). The extent of this asymmetry is summarized for several GPS PRNs in Figure 2.

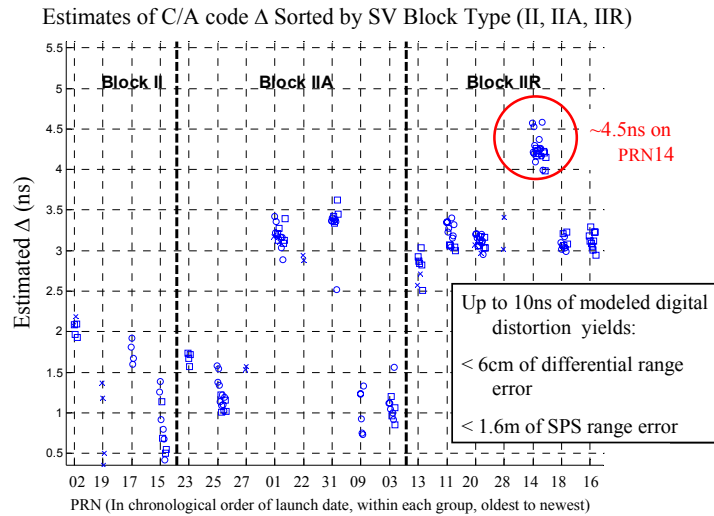


**Figure 2.** High-resolution measurements of lead/lag (digital) code distortion on several GPS PRNs (Mitelman, 2005).

Two key observations in Figure 2 should be noted. First, none of the PRN codes have a digital distortion equal to zero; none of the broadcast codes are ideal. Second, the largest deformation of this type was approximately 4.5ns and was observed on PRN 14. PRN14 is broadcast on SV14—a relatively new, Block IIR SV. Ironically, the older SVs have relatively smaller, but still non-zero, digital distortion (1-2ns). Figure 2 confirms that modeling the GPS ranging signals as ideal PRN codes is not precisely correct. Still, it does not provide insight into other types of deformation (e.g., analog or filter-induced distortions) that may be present on the signals.

Note that the position errors one might expect due to these nominal deformations will vary depending on the specific satellites included in a given navigation solution. However, if the code asymmetry is as large as 10ns on a single SV ranging signal, and all others are ideal and have no lead/lag distortion—as assumed by Phelts, *et al* (2000) and by Macabiau and Chatre (2000) for traditional signal quality monitoring (SQM) analysis—the SPS range errors may be as large as 1.6 meters. For differential users, such as those who use the Local Area Augmentation System, the errors may be as large as 6cm. (The details of this particular SQM analysis are beyond the scope of this paper.)

### 2.4.1 Correlation Domain Observations

Differences in correlation peak measurements can easily be verified with a more-conventional GPS receiver-antenna setup (Brenner *et al*, 2002). Figure 3 shows an overlay of eight

correlator outputs from a single multi-correlator receiver (having a 16MHz front end bandwidth) tracking 12 GPS SVs. The correlator offsets are spaced at approximate code chip offsets of (from early-to-late, in units of C/A code chips): -0.1023 -0.076 -0.05115 -0.025 +0.025 +0.05115 +0.076 +0.1023. To reduce the effects of multipath, approximately 1.5-2 hours of high-elevation ( $>60^\circ$ ) measurements were averaged for each SV signal. Each correlation measurement is normalized to the early side of the uppermost pair ( $\pm 0.025$  chips). (Since this pair was used as the tracking pair, the values at both the -0.025 and +0.025 outputs were nearly equal at all times.) The PRNs under consideration included: 1, 5, 13, 14, 18, 20, 23, 25, 27, 28, and 30. Any PRNs that produced ideal peaks of greater or lesser slope than these were excluded.

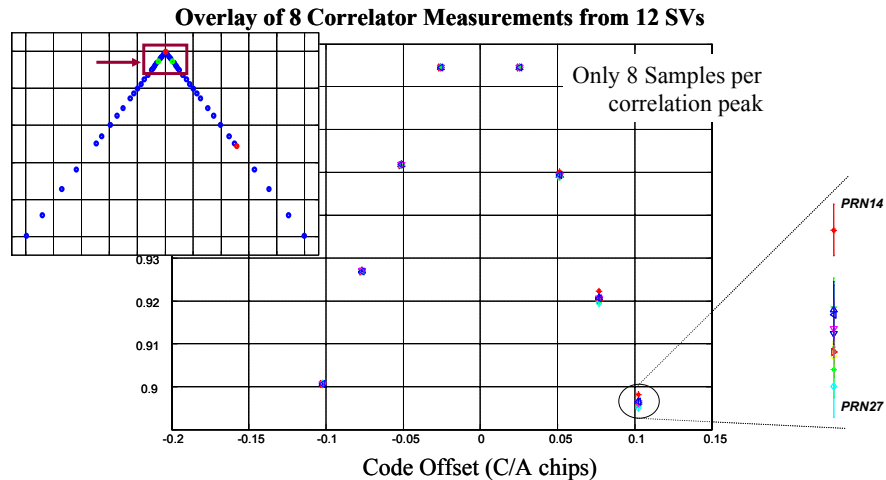


**Figure 3.** Correlator outputs from a 16MHz receiver, having 12-channels and 8 correlators per channel. The measurements from 12 SVs were time-averaged then compared to each other.

From the figure, it is readily apparent that the correlation peak does not appear symmetric simply due to receiver filtering and some residual multipath effects. However, this is not the primary concern since the filter effects should affect identical signals identically. The figure confirms two key things. First, the correlation peaks differ from one to another. Since the receiver filter itself is applied the same to all incoming signals, the incident signals themselves must be distorted differently. Second, the peak corresponding to PRN14 produced the largest deviation from the others. This corresponds with the digital code measurement data discussed previously. This correlation peak comparison, however, is more comprehensive; it includes any analog/filter distorting effects as well.

### 3. ANALYSIS

#### 3.1 Ideal Correlation Peaks

A normalized, ideal correlation peak for the current GPS C/A codes may be modeled as

$$R(\tau) = \begin{cases} 1 - \frac{|(1 - \kappa)\tau|}{T_c} & |\tau| \leq T_c \\ \kappa & \text{otherwise} \end{cases} \quad (1)$$

Where  $T_c$  is one C/A code chip period and  $\kappa$  is a constant corresponding to the slope of the

correlation peak. And, for a nominal (Type 1) peak,  $\kappa = \kappa_{(1)} = -1/1023$ . However, it may also be  $-65/1023$  or  $63/1023$ —corresponding to a “skinny” (Type 0) or “broad” (Type 2) peak, respectively. Note that as these are simple linear slope variations that do not affect correlation peak symmetry; tracking errors are virtually unaffected by these slope differences.

For direct comparisons of correlation peaks of different types, they may be effectively removed or calibrated by a simple linear conversion. For example, to convert from a correlation peak type  $\zeta$  to a Type 1 (or nominal) peak, the following equation may be used:

$${}_{(\zeta) \rightarrow (1)} R(\tau) = {}_{(\zeta) \rightarrow (1)} R(\tau) + |\tau|(\kappa_1 - \kappa_\zeta)$$

where

$$\kappa_{(0)} = -65/1023 \tag{2}$$

$$\kappa_{(1)} = -1/1023$$

$$\kappa_{(2)} = 63/1023$$

Table 1 summarizes the peak Types for 32 GPS PRNs. (The WAAS GEO ranging codes, PRN122 and PRN134, are both Type 1.) Unless otherwise mentioned, this paper assumes and compares Type 1 correlation peaks. If any PRNs from Types 0 or Type 2 are referenced, their slope differences were calibrated according to Equation 2 to match to nominal (Type 1) peaks.

Type	Description	PRN Numbers
0	“Skinny”	8, 22
1	Nominal	1,2,3,4,5,6,9,10,11,12,13,14,16,18,19,20,23,25,26,27,28,29,30,31,32
2	“Broad”	7, 15, 17, 21 24

**Table 1.** Correlation Peak Types of Current GPS PRNs

### 3.2 Filter Effects on Correlation Peaks

If the ideal correlation peak is given by Equation 1, the filtered correlation peak—as measured by the receiver—may be modeled as the convolution of multiple filters with the ideal peak. In traditional analyses, only the user segment filters are considered. If the front end filters of the receiver and the receiver antenna may be lumped into a single impulse response,  $h_{rx}$ , this equation is simply

$$R_{rx}(\tau) = h_{rx} * R(\tau) \tag{3}$$

If, however, all nominal satellite-induced distortions are included and are modeled as a single filter response parameter,  $h_{SV}$ , the equation for a single correlation peak becomes

$$R_{rx}(\tau) = h_{SV} * h_{rx} * R(\tau) \tag{4}$$

In Equation 4,  $h_{SV}$  accounts for both analog and digital distortion effects, since the digital distortion components (i.e., correlation peak dead zones) are assumed to be small relative to the effect of filter band limiting. (See Figures 1 and 2.) Equation 4 implies that differences in SV signal-generating hardware and filtering components will create *differences in correlation*

peak shape that are not generally considered in traditional code-tracking performance analyses. This may lead to navigation errors.

#### 4. EXPERIMENTAL SETUP

To identify and quantify the nominal deformation differences between GPS satellites, high-gain measurements were taken using the 46-meter parabolic dish antenna at Stanford University. The antenna achieves a 45dB gain and also incorporates a 50dB low-noise amplifier ( $T_{eq} \approx 40K$ ). It has a 50MHz bandwidth over the L-band. (See Figure 4.) This is the same antenna that was used to take the code distortion measurements of Figure 2.



**Figure 4.** High-gain parabolic radio telescope antenna used to acquire low-noise, wide bandwidth samples of the GPS signals.

Digital samples of the signals were taken using an Agilent 89640 Variable Spectrum Analyzer (VSA). It has a 36MHz span and was tuned to a center frequency of  $L1 = 1575.42MHz$ . It sampled the signals at 92.16MHz; this translates to a net sample rate of 46.08 samples/sec for both the in-phase and quadrature signal components. (Figure 5 shows a block diagram of the VSA.) These samples were, in turn, processed by a software radio receiver. (See Figure 6.) In this setup, the VSA—instead of a GPS receiver—provided the digitized samples to the software radio PC.

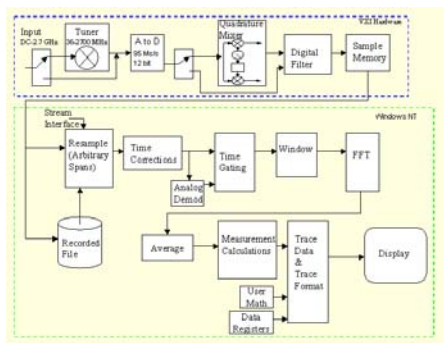


**Figure 5.** Block diagram of the Variable Spectrum Analyzer used to digitize the GPS signals

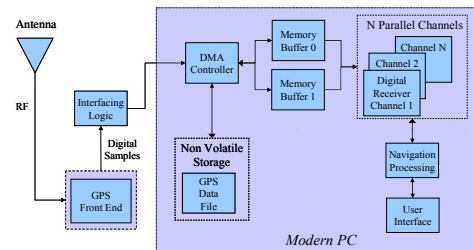


**Figure 6.** Block Diagram of the software radio receiver used to acquire and track the digitized GPS signals.



## 5. RESULTS

The test setup was used to analyze (in post-processing) five GPS satellite signals. The ranging signals of the two WAAS GEO signals were also processed for comparison. Figures 7 and 8 show the power spectra of PRN14 and PRN15 as measured by the SU Dish. The wide bandwidth of the antenna and VSA as well as the high gain of the antenna allows us to see the full GPS spectrum at L1. Only 250ms of data were used and averaged in these results. (This translated to 250 coherently-averaged correlation peaks.) Still, both lobes of the P(Y) code are visible, as is the center of the C/A code spectrum—above the center of the main lobe.

Figures 7 and 8 show the spectra for the WAAS GEOs AOR-W and POR. Since the GEOs only broadcast the C/A code (at L1) and bandwidth of these signals is limited to 2.2MHz, only the main lobes are visible. (The visible difference in the noise floor levels between the GPS and GEO spectra are due to the absence of automatic gain control stage on the front end of the spectrum analyzer.)

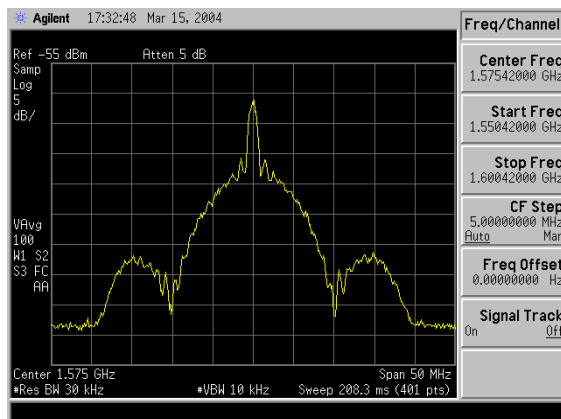


Figure 7. Measured Power spectrum of PRN14

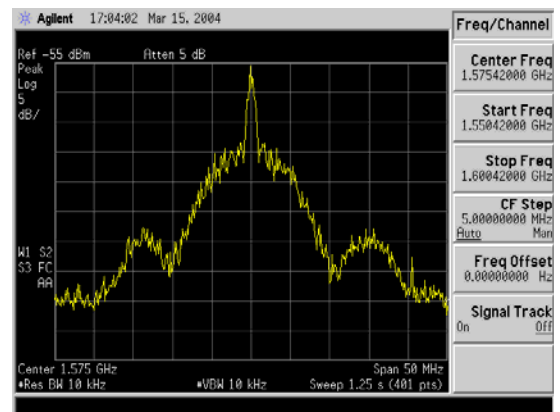


Figure 8. Measured Power spectrum of PRN14

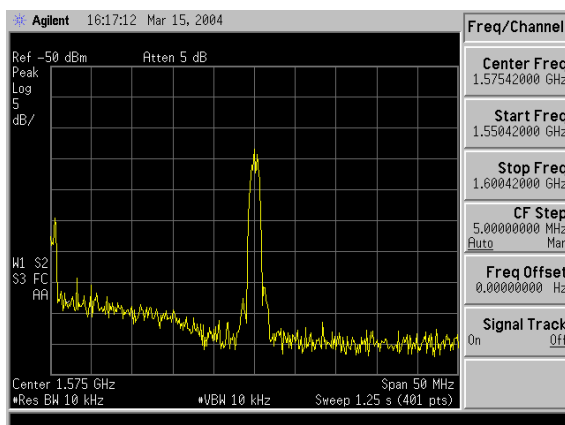


Figure 9. Measured power spectrum of a WAAS geostationary satellite: AOR-W

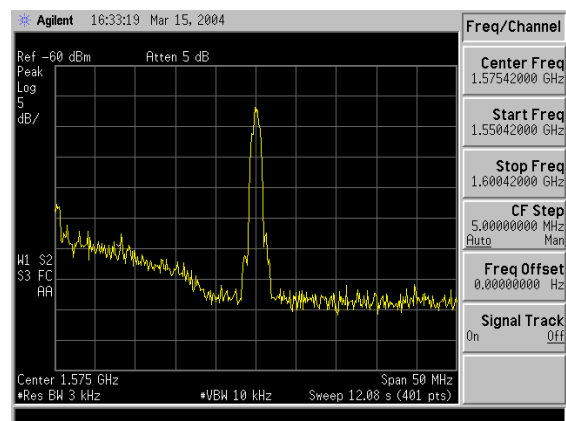
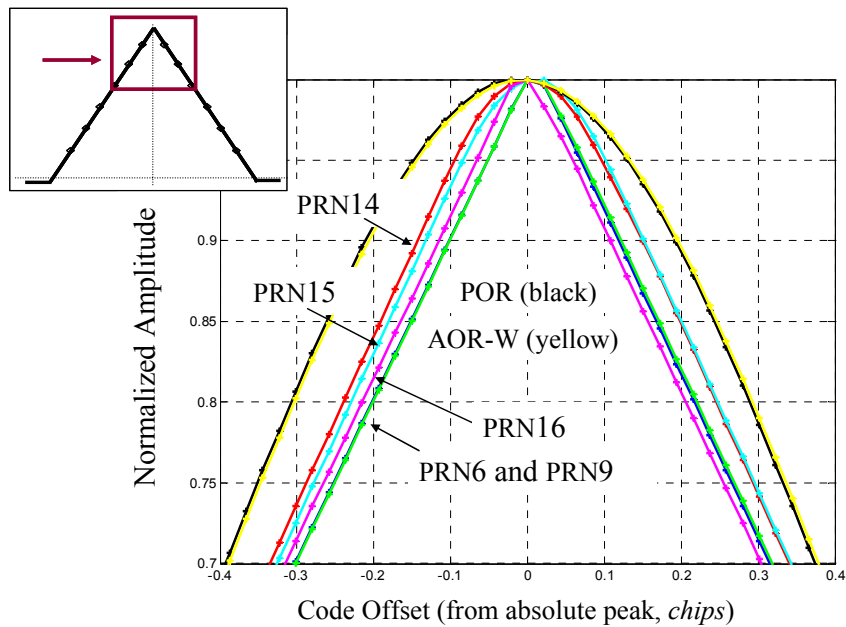


Figure 10. Measured power spectrum of a WAAS geostationary satellite: POR

An overlay of the correlation peaks corresponding to PRNs 6, 9, 14, 15, 16 and the two WAAS GEOs (PRN122 and PRN134) are shown in Figure 11. Only the uppermost portions of the peaks are shown. Their correlation amplitudes are normalized relative to their respective maxima (i.e., their absolute peaks). Note that since, in this general case, the true code offsets are unknowns, each peak was centered relative to these maxima.

Immediately from the plot, several key observations may be made. First, as expected, distortion due to thermal noise and multipath is negligible on these peaks. The high-gain dish measurements are extremely clean (Akos *et al*, 2004). Second, none of the peaks have infinite bandwidth. The severe rounding of the GEO peaks due to the 2.2MHz filter present in the GEO signal transmission chain is also as expected. However, relatively notable rounding is noticeable on several GPS peaks as well. Third, the all of the correlation peaks have distortion that differs relative to each other. Some deviations from the ideal triangular peak are expected due to the presence of the small amount of filtering induced by the antenna. However, there are significant *relative difference in correlation peak symmetry* that can only explained by differences in the signal filtering and transmission characteristics of the satellites themselves.



**Figure 11.** Correlation peak comparison of five GPS PRNs. The relative differences between the peaks is readily apparent and is due to differences in the transmission path characteristics of the satellites. Correlation peaks corresponding to the two WAAS GEO signals are also shown for comparison.

A quantitative measure of the impact of these asymmetries lies in an analysis of resulting tracking errors. From these peaks, the differential tracking errors from each PRN relative to a single correlator spacing may be found. Recall that the absolute tracking error (or code offsets) cannot be determined without the presence of an ideal, undistorted peak to use as a reference. Still, for high-accuracy and high-integrity systems such as LAAS, maximum differential range errors are of primary concern. These errors are explored in more detail below.

The early-minus-late tracking errors,  $\tau$ , for any correlator spacing  $d$  is easily found as a

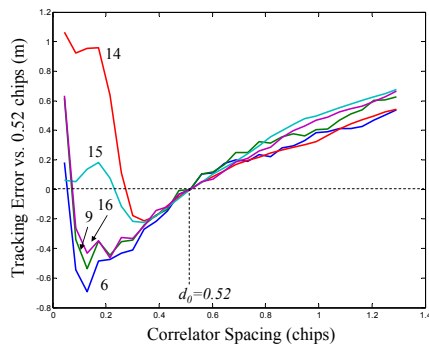
solution to the following equation:

$$\tau(d) = \arg\{R_{rx}(\tau + d/2) - R_{rx}(\tau - d/2) = 0\} \quad (5)$$

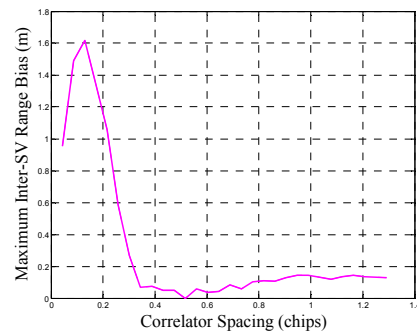
Using Equation 5, Figure 12 plots the result for each of the five GPS correlation peaks where the reference correlator spacing was  $d=0.52$  chips. A perfectly symmetric peak would be a horizontal line placed at 0m—indicating a differential range error of zero meters for all correlator spacings. An asymmetric peak produces a variable range error as a function of correlator spacing. If all SV signals transmitted identically-distorted signals, all five curves would overlap. The variation between curves indicates the degree to which the nominally distorted SVs differ. Larger variations indicate the potential for larger range errors.

Figure 13 quantifies the maximum spread of the traces in Figure 12 as the maximum nominal inter-SV range bias. This is a pessimistic estimate, of course, based on these five signal measurements. It presumes that a receiver may acquire several SVs such that all of the bias is effectively contained in a single range measurement. For example, in the case of Figure 13, a receiver having a correlator spacing of 0.1 may have approximately 1.5 meters of error if it tracks 3 signals similar to PRN6 and only one similar to PRN14.

For this reference spacing, the plot reveals that the nominal range errors for a user receiver having a correlator spacing greater than 0.52 would be relatively small. (It is identically zero, of course, at  $d = d_{user} = 0.52$  chips.) Still, the differences are not negligible and are not easily predicted without these types of correlation peak measurements.



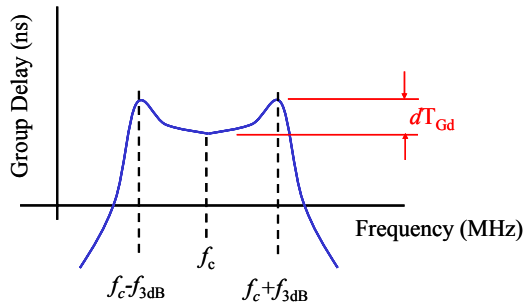
**Figure 12.** Comparison of relative differential tracking errors of five GPS PRNs. The errors are referenced to the tracking error at a correlator spacing of 0.52 chips.



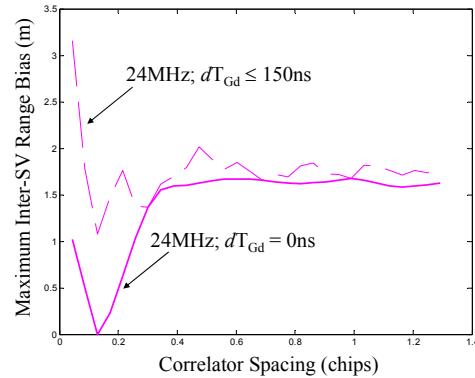
**Figure 13.** Absolute maximum differential tracking error for five GPS PRNs. This curve computes an effective “worst-case” bias on a single range. It plots the magnitude of the difference between the maximum and minimum contours shown in Figure 12.

In the above examples, the effective user receiver bandwidth was that of the parabolic antenna system (i.e.,  $> 40\text{MHz}$ ). More realistically, current GPS receivers have bandwidths of  $24\text{MHz}$  or less. Also, user receiver filters have differential group delays that will create signal distortion. (See Figure 14.) Since the GPS signals are not identical, receiver filter group delays will modify and, in general, increase whatever distortion is present on the incoming signals. A conservative model of a receiver filter group delay profile is shown in Figure 14. (This type of filter group delay response and its effects on range errors is discussed more completely by Phelts *et al* (2004).)

A LAAS user receiver, for example, with a bandwidth of 24MHz may have a differential group delay that varies by as much as 150ns. User avionics receivers will generally have some unknown (but bounded) differential group delay,  $dT_{Gd} \neq 0$ ns. So their range errors will not always differentially cancel—even at a correlator spacings matched to that of the LGF receivers. The dashed curve in Figure 15 illustrates this case for a 24MHz reference receiver with a correlator spacing of approximately 0.082 chips. (For simplicity, the reference receivers was assumed to have  $dT_{Gd} = 0$ ns.)



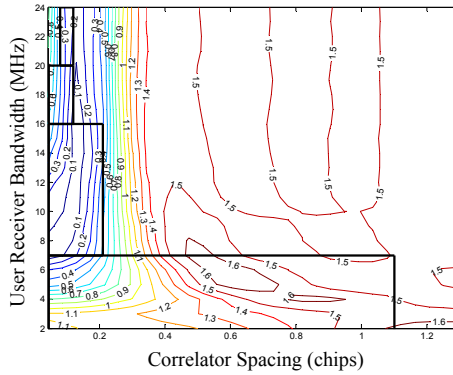
**Figure 14.** Illustration of a symmetric, parabolic group delay response profile. The differential group delay parameter is a measure of the maximum passband group delay variation.



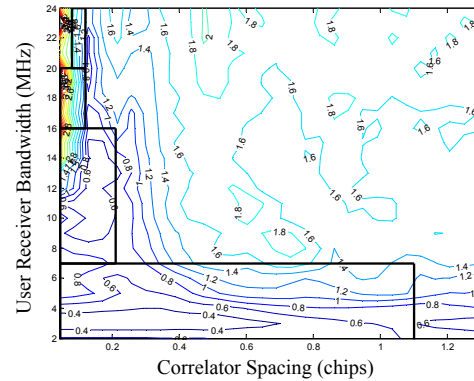
**Figure 15.** Absolute maximum differential tracking error for five GPS PRNs assuming a 24MHz reference receiver (with  $dT_{Gd} = 0$ ns) and several 24MHz-user receivers with  $0 \leq dT_{Gd} \leq 150$ ns. (The dashed line represents the user with the group delay that yielded the maximum error.)

Figure 15 shows that when  $dT_{Gd} = 0$ ns and the bandwidth is limited to 24MHz the maximum error is still slightly greater than 1.5 meters. (As expected, the error is identically zero at the reference spacing of 0.082 chips.) In this case, the smaller maximum potential errors occur for narrower correlator spacings. After applying the differential group delay variation—from to 150ns in 25ns increments—the maximum error (over all differential group delays within the stated range) increased to more than 3 meters. Under these conditions, the largest potential biases occur for the receivers with narrowest correlator spacings.

Figures 16 and 17 generalize this example for receivers of narrower, more-practical front end bandwidths; the reference receiver for both had a 16MHz bandwidth. Figure 16 illustrates the case for  $dT_{Gd} = 0$ ns and Figure 17 shows the case for  $dT_{Gd} \leq 150$ ns. For the former, the error is identically zero where that the correlator spacings are matched (at 16MHz and  $d=0.082$  chips). The biases are never zero in Figure 17, however. They are largest—approximately 5 meters—for the narrowest correlator spacings and widest bandwidths. The smallest (~50cm or less) errors occur for receivers with narrower bandwidths combined with relatively narrow correlator spacings. The regions outlined in black indicate the design configurations allowed by LAAS and WAAS.



**Figure 16.** Absolute maximum differential tracking errors for five GPS PRNs assuming a 24MHz reference receiver (with  $dT_{Gd} = 0\text{ns}$  and  $d = 0.82$ ) and various user receiver configurations with  $dT_{Gd}=0\text{ns}$ . Regions outlined in black indicate configurations valid for LAAS (and WAAS).



**Figure 17.** Absolute maximum differential tracking errors for five GPS PRNs assuming a 16MHz reference receiver (with  $dT_{Gd} = 0\text{ns}$  and  $d = 0.82$ ) and various user receiver configurations with  $0 \leq dT_{Gd} \leq 150\text{ns}$ . Regions outlined in black indicate configurations valid for LAAS (and WAAS).

Several points should be noted when considering these results. The reference spacing of 0.082 chips is not matched to that of a true LAAS or WAAS reference receivers. No interpolations were used; specific spacings selected in this paper are not exact due to finite sampling resolution of the measurement hardware. Also, in actual differential GPS systems, the reference receivers themselves have group delay effects that may impact these results. Finally, the analysis of this paper does not represent a rigorous integrity analysis for LAAS or WAAS. It simply serves as an indicator of this potential issue for consideration in the design of these systems.

## 6. SUMMARY AND CONCLUSIONS

These results verify that the GPS signals are not ideal. Nominal distortions present on the signals are not only present but they may vary from SV-to-SV. Further, receiver filter group delay specifications have a significant effect on the potential magnitude of these biases. It may be a much more important parameter to consider for receiver designs than is generally assumed. These conclusions can be reached from analyzing a relatively small sampling of SVs. Accordingly, this implies that the true distribution of potential range errors may vary more widely than this paper suggests.

The analysis above still presents a relatively conservative view of these biases. (This was necessary, in part, due to the very limited amount of SV data available.) In practice, their effect on navigation performance may be significantly smaller for two reasons. First, in general, position solutions are found using a relatively large of different satellite signals—each contributing a different degree of distortion. Effective range errors—and, hence, position errors are likely relatively small as a result. Second, the group delay effects of the filters in most quality receivers likely have much smaller impact on code distortion than was modeled here.

More work in this area is required to verify these results and make them more useful to the GPS community. For one, a more detailed calibration of the antenna used should be

performed. Also, additional SVs should be measured and compared to the others. For LAAS (and WAAS), augmentation system-specific details (e.g., receiver architectures and reasonable group-delay profiles) should be correctly modeled and integrated into the analysis. Finally, further attempts should be made to isolate, measure and identify this error source—using real data—in the range and position domains.

## REFERENCES

- Akos DM, Mitelman A, Phelts RE, Enge P, (2004) *High Gain Antenna Measurements and Signal Characterization of the GPS Satellites*, Proceedings of the 2002 17<sup>th</sup> International Technical Meeting of the Satellite Division of the Institute of Navigation, ION GNSS-2004.
- Brenner M, Kline P, Reuter R, (2002) *Performance of a Prototype Local Area Augmentation System (LAAS) Ground Installation*, Proceedings of the 2002 15<sup>th</sup> International Technical Meeting of the Satellite Division of the Institute of Navigation, ION GPS/GNSS-2002.
- Edgar C, Czopek F, Barker B (2000) *A Co-operative Anomaly Resolution on PRN-19*, Proceedings of the 2000 13<sup>th</sup> International Technical Meeting of the Satellite Division of the Institute of Navigation, ION GPS-2000. Proceedings of ION GPS 2000, v 2, pp. 2269-271.
- Enge PK, Phelts RE, Mitelman AM, (1999) *Detecting Anomalous signals from GPS Satellites*, ICAO, GNSS/P, Toulouse, France.
- Macabiau C, Chatre E (2000) *Impact of Evil Waveforms on GBAS Performance*, Position Location and Navigation Symposium, IEEE PLANS, pp. 22-9.
- Mitelman AM (2005) *Signal Quality Monitoring For GPS Augmentation Systems*, Ph.D. Thesis, Stanford University, Stanford, CA.
- Mitelman AM, Phelts RE, Akos DM, Pullen SP, Enge PK (2000) *A Real-Time Signal Quality Monitor for GPS Augmentation Systems*, Proceedings of the 13<sup>th</sup> International Technical Meeting of the Satellite Division of the Institute of Navigation, ION-GPS-2000, pp. 177-84.
- Phelts, RE (2001) *Multicorrelator Techniques for Robust Mitigation of Threats to GPS Signal Quality*, Ph.D. Thesis, Stanford University, Stanford, CA.
- Phelts RE, Akos DM, Enge PK (2000) *Robust Signal Quality Monitoring and Detection of Evil Waveforms*, Proceedings of the 13<sup>th</sup> International Technical Meeting of the Satellite Division of the Institute of Navigation, ION-GPS-2000, pp. 1180-1190.
- Phelts RE, Walter T, Enge PK (2004) *Range Biases on the WAAS Geostationary Satellites*, Proceedings of the 2004 National Technical Meeting, Institute of Navigation.